Identification of compounds with cytotoxic activity from the leaf of the Nigerian medicinal plant, *Anacardium occidentale* L. (Anacardiaceae)

Bamigboye J. Taiwo*[a,b], Amos A. Fatokun*[b]#, Olujide O. Olubiyi[a], Olukemi T. Bamigboye-Taiwo[c,d], Fanie R. van Herdeen[e] and Colin W. Wright[b]

[a]*Department of Pharmaceutical Chemistry, Faculty of Pharmacy, Obafemi Awolowo University, Ile Ife, Nigeria.*
[b]*School of Pharmacy, Faculty of Life Sciences, University of Bradford, Bradford BD7 1DP, England, United Kingdom.*
[c]*Department of Physiology, Faculty of Basic Medical Science, Obafemi Awolowo University, Ile Ife, Nigeria*.
[d]*Department of Paediatrics, Federal Teaching Hospital, Ido-Ekiti, Ekiti State, Nigeria.*
[e]*School of Chemistry and Physics, Pietermaritzburg Campus, University of KwaZulu-Natal, Private Bag X01, Scottsville 3209, South Africa*

*Corresponding authors: Bamigboye J. Taiwo (bamit@oauife.edu.ng or taiwobami2001@yahoo.com; Phone: +2348066507213), Amos A. Fatokun (A.A.Fatokun@ljmu.ac.uk; Phone: +44(0) 151 904 6291)

#Current address: School of Pharmacy and Biomolecular Sciences, Faculty of Science, James Parsons Building, Liverpool John Moores University, Byrom Street, Liverpool L3 3AF, UK

Abstract

Cancer is now the second-leading cause of mortality and morbidity, behind only heart disease, necessitating urgent development of (chemo)therapeutic interventions to stem the growing burden of cancer cases and cancer death. Plants represent a credible source of promising drug leads in this regard, with a long history of proven use in the indigenous treatment of cancer. This study therefore investigated *Anacardium occidentale*, one of the plants in a Nigerian Traditional Medicine formulation commonly used to manage cancerous diseases, for cytotoxic activity. Bioassay-guided fractionation, spectroscopy, Alamar blue fluorescence-based viability assay in cultured HeLa cells and microscopy were used. Four compounds, zoapatanolide A (**1**), agathisflavone (**2**), 1,2-bis(2,6-dimethoxy-4-methoxycarbonylphenyl)ethane (anacardicin, **3**) and methyl gallate (**4**), were isolated, with the most potent being zoapatanolide A with an IC_{50} value of 36.2 ± 9.8 µM in the viability assay. To gain an insight into the likely molecular basis of their

observed cytotoxic effects, Autodock Vina binding free energies of each of the isolated compounds with seven molecular targets implicated in cancer development (MAPK8, MAPK10, MAP3K12, MAPK3, MAPK1, MAPK7 and VEGF), were calculated. Pearson correlation coefficients were obtained with experimentally-determined IC_{50} in the Alamar blue viability assay. While these compounds were not as potent as a standard anticancer compound, doxorubicin, the results provide reasonable evidence that the plant species contains compounds with cytotoxic activity. This study provides some evidence of why this plant is used ethnobotanically in anticancer herbal formulations and justifies investigating Nigerian medicinal plants highlighted in recent ethnobotanical surveys.

Key words: Cancer, Lead compound, Nigerian medicinal plants, Drug discovery, Cytotoxicity.

1. Introduction

Cancer is a leading cause of mortality and morbidity, behind only heart disease, with projected 1,685,210 new cancer cases and 595,690 cancer deaths in the United States alone in 2016,[1] while current treatments are being sub-optimal.[2,3] In low- and middle-income countries of the developing world, the growing burden of new cancer cases and cancer deaths is predicted to continue to worsen[4] thus requiring renewed global research effort in the development of more effective chemotherapeutic agents for cancer management and/or treatment. Plants have been a major component of Traditional Medicine (TM), a cultural heritage and system of indigenous wisdom adopted for several centuries to manage the health of people in most traditional societies. Plants largely represent a credible source of promising drug leads in this regard, as they have a long history of proven use[5-13] in the indigenous treatment of cancer,[14] *e.g.*, *Taxus breviflora* L. (Taxaceae),[15,16] *Podophylum peltatum* L. (Beberidaceae),[17] *Catharanthus roseus* G. Don (Apocyanaceae),[18] *Raphanus sativus* L. (Cruciferae),[19,20] *Combretrum caffrum* (Eckl. & Zeyh.) Kuntze (Combretaceae),[21] *etc*. There is currently a global renaissance of ethnobotanical surveys of medicinal plants in traditional societies, most especially in China and India, seeking to identify plants having potential anti-inflammatory and anticancer activities, amongst other activities. In Nigeria, there have been some ethnobotanical surveys of medicinal plants used in cancer treatment.[22-26] This has encouraged research into some of these plants in order to discover any scientific justification for their ethnobotanical uses. We have been active in this effort, and the study herein reported was initiated as a continuation of our study on Nigerian medicinal plants.[27]

From our interactions with the traditional medical practitioners (TMPs), a herbal formulation used for the treatment of cancerous diseases was volunteered (personal communication). The

formula for the herbal formulation is as follows: 'Whole plant of *Synedrella nodiflora* L. Gaertn (Asteraceae), the leaves of *Alafia barteri* Oliv. (Apocyanaceae), the leaves of *Anacardium occidentale* L. (Anacardiaceae) and the aerial parts of *Cardiospermum grandiflorum* Sw. Sapindaceae) were boiled with water and a tumbler (*ca* 200 mL) is to be taken three times daily for six months'. This study used a bioactivity-guided approach, which revealed active extracts and fractions from which compounds were isolated. We report the identification of four compounds (**1-4**) from *A. occidentale*, one of the plant constituents of the herbal formulation, and the assessment of their potential to kill cancer cells. The binding free energies of each compound with target proteins were also calculated and Pearson correlation coefficients were plotted using experimentally-obtained IC_{50} values.

2. Results and discussion

2.1. Structural elucidation of isolated compounds from A. occidentale

The crude absolute ethanolic extract of *A. occidentale* was subjected to chromatographic fractionation on silica gel mesh 200-400 and activity was determined using the Alamar Blue cell viability assay. The HeLa cell line, a widely-used model of cervical cancer, was used in the bioassay-guided isolation of compounds. Four compounds (**1-4**) were isolated as cytotoxic principles from the crude leaf extract (Figure 1).

2.1.1. **Compound 1** was isolated as a grey-white powder. The proton spectrum showed four methyl signals at δ_H 1.98 (3H, H-4'), 1.91 (3H, H-14), 1.90 (3H, H-5') and 1.80 ppm (3H, H-15). There were two methylene signals at δ_H 2.69 (1H, m, H-2a) and 2.20 (1H, m, H-2b), both observed to be attached to δ_C 32.4 (C-2) in the HSQC spectrum. An aliphatic methine signal was

observed at δ_H 2.81 (dd, *J* = 9.8, 1.3 Hz, H-7), attached to δ_C 48.3 ppm (C-7) also in the HSQC spectrum. Four deshielded methine signals were observed at δ_H 4.15 (1H, d, *J* = 9.4 Hz, H-9), 4.72 (1H, t, H-3), 4.78 (1H, d, *J* = 10.9 Hz, H-6) and 5.01 (1H, t, H-8). The remaining signals were observed as olefinic proton signals at δ_H 5.11 (1H, d, *J* = 10.6 Hz, H-5), 5.36 (1H, t, H-1), 5.64 (1H, d, *J* = 1.3 Hz, H-13a) and 6.31 (1H, d, *J* = 1.3 Hz, H-13b). Cross peaks were observed in the COSY spectrum between the signals at δ_H 2.81 and δ_H 6.31, 5.64, 5.01; at δ_H 4.75 and δ_H 2.69, 2.17; at δ_H 4.78 and δ_H 5.12; at δ_H 5.35 and δ_H 2.67, 2.25; at δ_H 5.01 and δ_H 4.16, 2.81. The carbon-13 and DEPT spectra revealed 20 signals in all at δ_C 169.2 (Cq, C-12), 166.9 (Cq, C-1'), 141.0 (CH, C-2'), 140.7 (Cq, C-12), 135.5 (2Cq, C-4, 10), 126.9 (=CH_2, C-13), 126.7 (CH, C-3'), 124.7 (CH, C-5), 123.3 (CH, C-1), 80.6 (CH, C-9), 75.5 (CH, C-6), 72.9 (CH, C-8), 67.7 (CH, C-3), 48.5 (CH, C-7), 32.4 (CH_2, C-2), 20.4 (CH_3, C-5'), 17.3 (CH_3, C-15), 16.0 (CH_3, C-4') and 11.8 (CH_3, C-14). In the HMBC spectrum, long range correlation was observed between the proton signal at δ_H 1.80 and the carbon signals at δ_C 67.7, 123.3 and 141.4. Also, long range correlations were observed between the following set of signals: δ_H 1.90 and δ_C 80.6, 124.7, 135.5; δ_H 1.91 and δ_C 126.7, 140.7, 166.9; δ_H 1.98 and δ_C 140.7, 126.9; δ_H 5.01 and δ_C 80.8; δ_H 5.11 and δ_C 75.6; δ_H 5.64 and δ_C 169.2 and finally between δ_H 6.30 and δ_C 48.5, 169.2. The NMR spectrum suggested a germacrane framework (δ_H 1.89, s, Me-14 and δ_H 1.79 d, *J* = 1.5 Hz, Me-15) with oxygenated functions at C-3, C-6, C-8, and C-9, while an α-methylene-γ-lactone [δ_C 169.2 (C-12), 135.5 (C-11), and 126.0 (C-13); δ_H 5.67 and 6.30 (H-13)] was also evident. The remaining signals were from the esterification with angelic acid, with the total number of carbon atoms being 20. The molecular formula for **1** was indicated from the LTQ Orbitrap XL FTMS as $C_{20}H_{26}O_6$ from mass spectrum signal at *m/z* of 747.3351 $[2M+Na]^+$ (calculated mass 747.3351 for $C_{40}H_{52}O_{12}Na$) for the sodiated dimeric adduct. The ^1H NMR data were in good agreement

with that obtained for the heliangolide, zoapatanolide A, isolated from *Montana tomentosa*[28,29,30] and we herein present its carbon-13 data for the first time. Therefore, **1** was identified as zoapatanolide A. To the best of our knowledge, this is the first report of a sesquiterpene α-methylene-γ-lactone from Anacardiaceae.

2.1.2. **Compound 2** was isolated as a yellow amorphous powder. ESI-MS spectrum gave a peak at *m/z* 561 $[M+Na]^+$. The NMR data of **2** (Section 2.2) when compared with literature data[31,32] allowed the assignment of **2** as agathisflavone.

2.1.3. **Compound 3** was isolated as a greyish white powder. The molecular formula of $C_{22}H_{26}O_8$ was determined based on the HR ESI-Q-TOF MS at *m/z* 441.1529 $[M+Na]^+$ (calculated for $C_{22}H_{26}O_8Na$, 441.1525). In the HSQC spectrum, the proton signal at δ_H 3.82 correlated with two carbon signals at δ_C 52.3 and 56.3, an indication of two overlapping proton signals at δ_H 3.82. These signals were observed to possess long-range correlation with the signals at δ_C 146.6 and 168.9 in the HMBC spectrum. Also, the signal at δ_H 7.03 was observed to correlate with the carbon signals at δ_C 109.8, 121.2, 146.6 and 168.9. However, the MS peak at *m/z* 441 $[M+Na]^+$ is for a molecular formula $C_{22}H_{26}O_8$, and a *m/z* unit twice the mass expected for a methyl 3,5-dimethoxyl-4-methylbenzoate, indicates the existence of a dimer. Thus, compound **3** is determined to be 1,2-bis(2,6-dimethoxy-4-methoxycarbonylphenyl)ethane (anacardicin). An analogue of this compound, 2,2-dicarboxy-4,4',5,5'-tetramethoxydibenzyl dimethyl ester, was synthesized by Battersby and Binks,[33] from pavine through the Hofmann degradation reaction.

2.1.4 **Compound 4** was isolated as a brown powder. The ESI-MS spectrum showed a peak at *m/z* 183 $[M-1]^+$. By comparison of the NMR data with literature data,[34] compound 4 was determined to be methyl gallate.

2.2. Spectroscopic data for compounds 1, 2, 3 and 4

2.2.1. **Zoapatanolide A (1**) was isolated as off-white amorphous powder. **m.p.** 195-196 °C**.** **$[\alpha]_D^{25}$** = -82.4° (*c* 0.18, MeOH). **IR** (υ_{max} cm^{-1}); 3315, 2942, 2830, 2040, 1686, 1605, 1448, 1412, 1021. **^{1}H NMR** (400 MHz, CD_3OD) δ_H 1.80 (3H, H-10''), 1.90 (3H, H-9''),1.91 (3H, H-7''), 1.98 (3H, H-8''), 2.20 (1H, m, H-4b'), 2.69 (1H, m, H-4a'), 2.81 (dd, *J* = 9.8, 1.3 Hz, H-4''), 4.15 (1H, d, *J* = 9.4 Hz, H-7'), 4.72 (1H, t, H-3'), 4.78 (1H, d, *J* = 10.9 Hz, H-3), 5.01 (1H, t, H-8), 5.11 (1H, d, *J* = 10.6 Hz, H-1'), 5.36 (1H, t, H-5'), 5.64 (1H, d, *J* = 1.3 Hz, H-3'') and 6.31 (1H, d, *J* = 1.3 Hz, H-5''). **^{13}C NMR** (100 MHz, CD_3OD) δ_C 169.2 (Cq, C-11), 166.9 (Cq, C-1'), 141.0 (Cq, C-2'), 140.7 (Cq, C-12), 135.5 (2Cq, C-4, 10), 126.9 (=CH_2, C-13), 126.7 (CH, C-3'), 124.7 (CH, C-5), 123.3 (CH, C-1), 80.6 (CH, C-9), 75.5 (CH, C-6), 72.9 (CH, C-8), 67.7 (CH, C-3), 48.5 (CH, C-7), 32.4 (CH_2, C-2), 20.4 (CH_3, C-5'), 17.3 (CH_3, C-15), 16.0 (CH_3, C-4') and 11.8 (CH_3, C-14). **LTQ Orbitrap XL FTMS** *m/z* 747.3351 $[2M+Na]^+$, *i.e.* the sodiate dimeric adduct of $C_{20}H_{26}O_6$ (cal. for $C_{40}H_{52}O_{12}Na$ 747.3351).

2.2.2. **Agathisflavone (2**) was isolated as yellow amorphous powder. **IR** (υ_{max} cm^{-1}); 3200, 2953, 2922, 2853, 2111, 1718, 1645, 1604, 1576, 1552. **^{1}H NMR (**400 MHz, CD_3OD**)** δ_H 7.91 (2H, d, *J* = 8.8 Hz, H-2'/6'), 7.55 (2H, d, *J* = 8.8 Hz, H-2'''/6'''), 6.96 (2H, d, *J* = 8.8 Hz, H-3',5'), 6.75 (2H, d, *J* = 8.8 Hz, H-3''',5'''), 6.70 (1H, s, H-8), 6.63 (1H, s, H-3''), 6.59 (1H, s, H-3''), 6.38 (1H, s, H-6''). **^{13}C NMR (**100 MHz, CD_3OD**)** δ_C 184.0 (Cq, C-4/C-4''), 166.3 (Cq, C-2/2''), 166.1

(Cq, C-9/9''), 164.2 (Cq, C-7/7''), 162.8 (Cq, 4'/4'''), 162.6 (Cq, 5/5''), 129.6 (CH, 2'/6'), 129.3 (CH, C-2'''/6'''), 123.4 (Cq, C-1'''), 123.4 (Cq, C-1'), 117.1 (CH, C-3'''/5'''), 116.9 (CH, C-3'/5'), 104.0 (CH, C-10/10''), 103.4 (CH, C-3'/3''), 99.9 (Cq, C-6/8'') and 94.6 (CH, C-6''/8). **LC ESI-MS** *m/z* 561 $[M+Na]^+$, 537 $[M-1]^+$.

2.2.3. **Anacardicin** [1,2-bis(2,6-dimethoxy-4-methoxycarbonylphenyl)ethane] **(3). ^{1}H NMR** (400 MHz, CD_3OD) δ_H 7.04 (4H, s, H-2/6, 2'/6'), 3.82 (OCH_3, s, H-8/8'), 3.82 (4-OCH_3, s, H-9/9', 10/10') and **^{13}C NMR** (100 MHz) δ_C 168.9 (Cq, C-7,7'), 146.6 (Cq, C-3/5, 3'/5'), 121.3 (Cq, C-1/4, 1'/4'), 109.8 (CH, C-2/6, 2'/ 6'), 56.3 (OCH_3, C-9/10, 9'/1'), 52.3 (OCH_3, C-8/8') and 30.6 (CH_2, C-11/11'). **HR ESI-Q-TOF MS** *m/z* 441.1529 $[M+Na]^+$ (calc. for $C_{22}H_{26}O_8Na$ 441.1525).

2.2.4. **Methyl gallate** (**4**). **^{1}H NMR** (400 MHz, CD_3OD) δ_H 3.72 (3H, s, OCH_3), 6.94 (2H, s, H-2/6). **^{13}C NMR** (100 MHz) δ_C 168.9 (Cq, C-7), 146.6 (Cq, C-3/5), 139.8 (Cq, C-4), 121.1 (Cq, C-1), 110.2 (CH, C-2/6), 52.3 (OCH_3, C-8). **LC ESI MS** *m/z* 183 $[M-1]^+$.

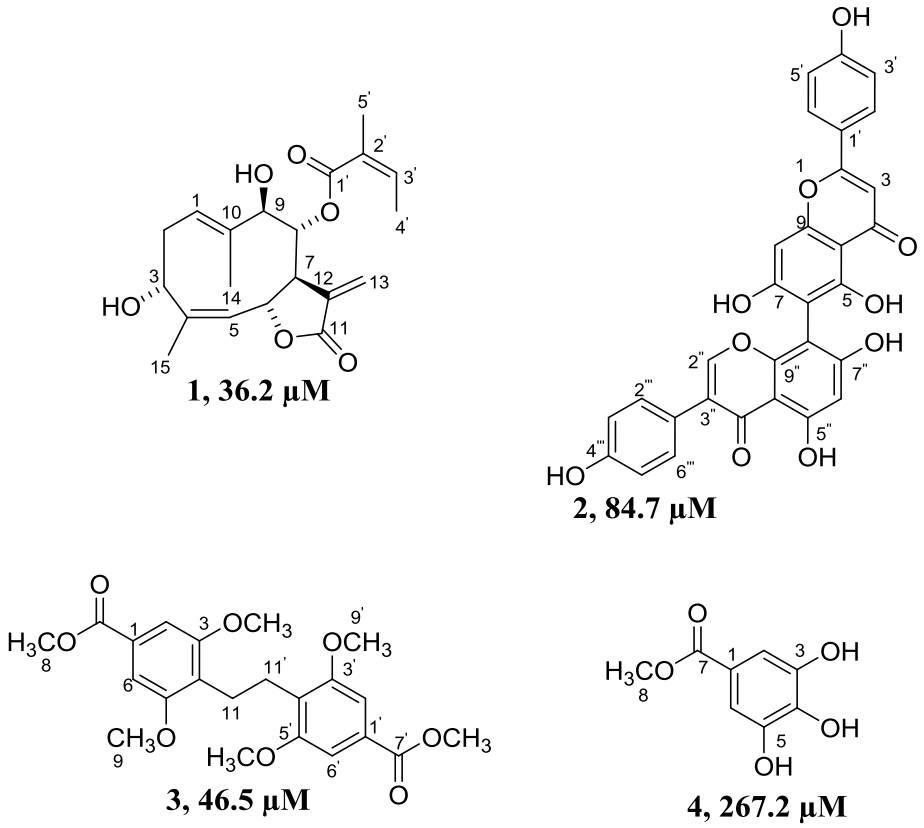

Figure 1. Structures of compounds **1-4** and their IC_{50} values.

2.3. Effects of extracts, fractions and isolated compounds on cell viability

Screening in HeLa cells was conducted sequentially, starting from acetone-soluble and acetone-insoluble extracts. The acetone-soluble extract showed activity while the acetone-precipitated extract did not show any activity. The acetone-soluble extract at 50 µg/mL and 100 µg/mL reduced HeLa cell viability to 90% and 9%, respectively, and was fractionated further on silica. The most potent fraction from the extract reduced viability to 35%. This was subjected to further purifications, producing fractions, the most potent of which achieved a reduction to 5% of cell viability at 100 µg/mL. Four compounds that showed activity were eventually isolated. The

effects of each of the four AO compounds on the viability of HeLa cells after 48 h incubation of the cultures with increasing concentrations of the compound up to 1.6 mM were then fully examined. The anticancer agent doxorubicin was used as a positive control and reference compound. Doxorubicin at 1, 2.5 and 5 µM yielded cell viability values of 106.5%, 50.8% and 40.0%, respectively (n=2) (IC_{50} circa 2.3 µM). All the test compounds elicited concentration-dependent reductions in HeLa cell viability but with varying potencies as revealed by their IC_{50} values, with the order of decreasing potencies being zoapatanolide **A** (**1**) (IC_{50} = 36.2 ± 9.8 µM) > anacardicin (**3**) (IC_{50} = 46.5 ± 4.1 µM) > agathisflavone (**2**) (IC_{50} = 84.7 ± 11.5 µM) > methyl gallate (**4**) (IC_{50} = 267.2 ± 29.4 µM) (Figure 2). For each compound, the degrees of reduction in cell viability correlated well with the extent of morphological damage seen in the corresponding photomicrographs. As compound concentrations were increased, there was greater loss of cells and more rounding up of the remaining cells. Representative photomicrographs for the most potent compound identified as zoapatanolide A (**1**), a sesquiterpene α-methylene-γ-lactone, are shown (Figure 3), compared to and contrasted with those of agathisflavone (**2**), which is less than half as potent. The cytotoxic potential of sesquiterpene α-methylene-γ-lactones had been well reported in literature.[35-37]

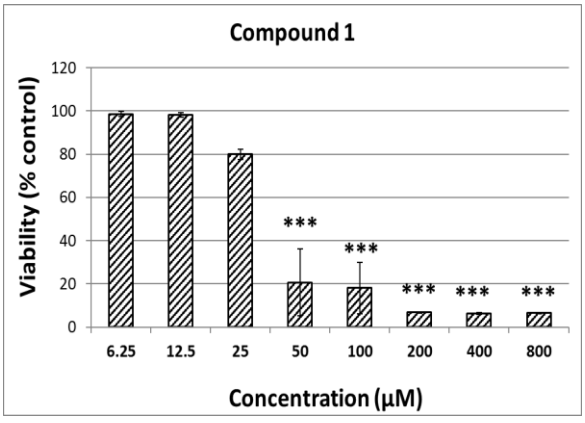

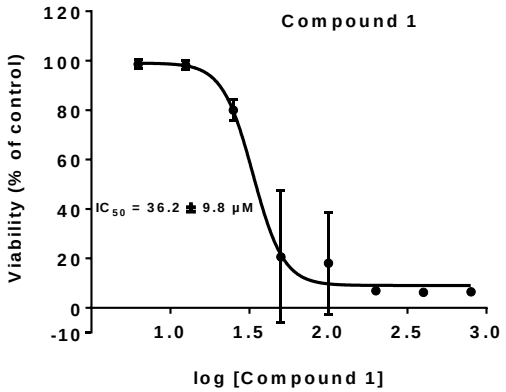

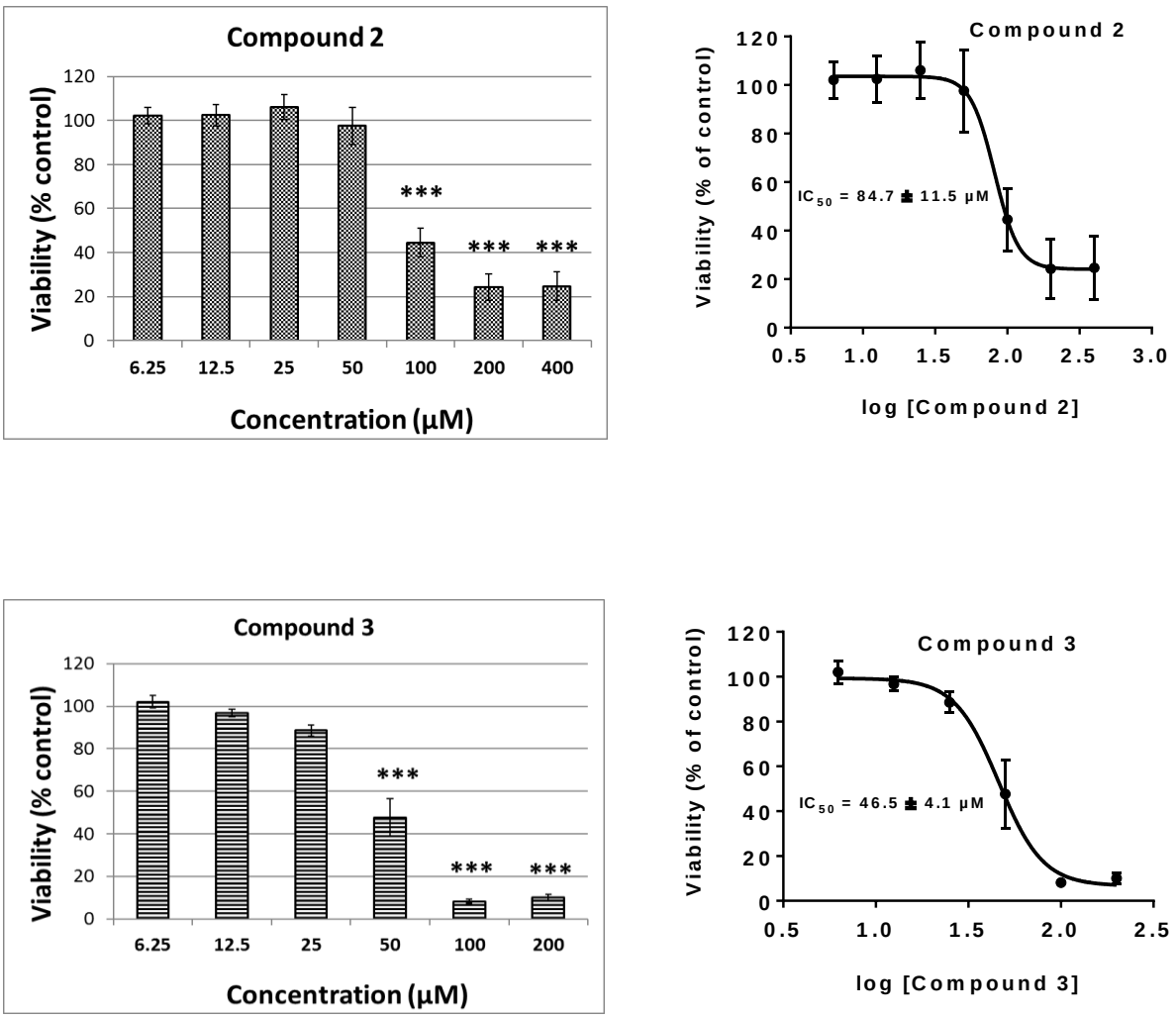

Figure 2. Concentration-dependent compound-induced reductions in HeLa cell viability (for compounds **1-3**). Cultures were incubated with a range of concentrations of the compounds for 48 h and viability was assessed using Alamar blue. Corresponding concentration-response curve fits for the calculation of IC_{50} values are also shown (IC_{50} values are as indicated on the curves). The IC_{50} value for compound **4** is 267.2 ± 29.4 µM (n=3-4). The anticancer agent doxorubicin was used as a positive control and reference sta ndard, with an estimated IC_{50} of approximately

2.3 μM. The rank order of increasing potencies of the compounds is zoapatanolide A (**1**) > anacardicin (**3**) > agathisflavone (**2**) > methyl gallate (**4**). ***P<0.001, compared to the negative control (DMSO only). Experiments were carried out at least three times (n=3 for **1** and **3** and n=4 for **2**).

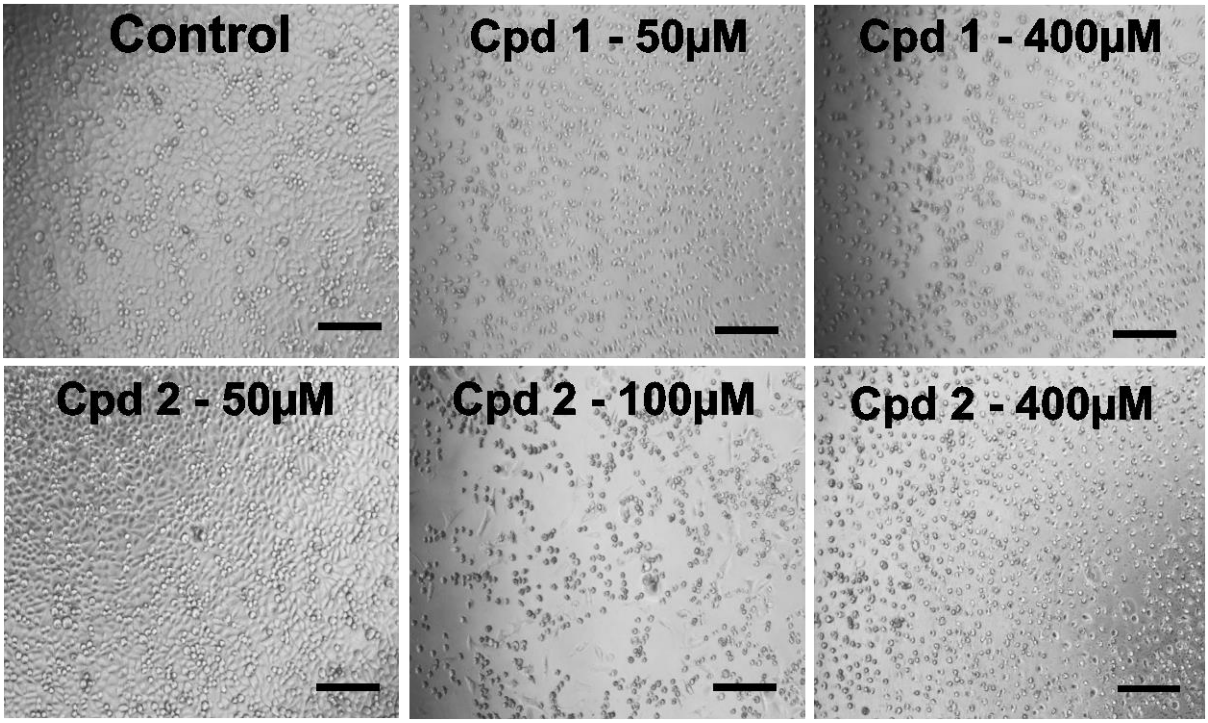

Figure 3. Effects of isolated compounds on the morphology of HeLa cells. Concentration-dependent damaging effects of representative compounds (abbreviated Cpd) zoapatanolide A (Cpd **1**) and agathisflavone (Cpd **2**) are compared and contrasted. Zoapatanolide A (Cpd **1**) is more than twice as potent as agathisflavone (Cpd **2**). For example, as shown, Cpd **1** at 50 μM caused significant damage to the cells whereas Cpd **2** at the same concentration elicited no significant damage. Damage was manifested by loss of cells and rounding up of remaining cells, compared to control cultures which were confluent and remained intact. Images were acquired,

following 48 h treatments, on a Nikon Eclipse TS100 inverted microscope (x10 magnification) fitted with a camera. Scale bar = 20 µm.

2.4. Computational studies on isolated compounds

All four compounds demonstrated strong binding to the seven protein targets, with the exemption of an unfavourable energetics computed for **2** against MAPK7. In most cases, the binding of **2** to the cancer drug targets suggests stronger interaction with the binding site residues than the interaction of each of the other three compounds. The highly favourable binding demonstrated by **2,** however, did not translate to the most potent cytotoxic activity. This could suggest the likely involvement of other molecular targets not included in the present study, or be due to unfavourable physicochemical properties that could limit the access of compound **2** to the receptor sites. To throw more light on this observed trend, molecular descriptors were computed for the four compounds and compared. $LogP_{(o/w)}$ values, molecular weights, and H-bond donor and H-bond acceptor values obtained for compounds **1**, **2**, **3** and **4** are, respectively: [1.8, 352.4, 3, 6], [5.4, 522.5, 5, 9], [3.9, 418.4, 0, 8], and [1.0, 184.1, 3, 6]. With $logP_{(o/w)}$ of 5.4, five (5) H-bond donors, nine (9) H-bond acceptors and molecular weight of 522.5, compound **2** has the most disadvantageous set of physicochemical properties. Thus, compared with the other screened compounds, the physicochemical properties of compound **2** are likely to render it less able to penetrate biological membranes to gain access to the receptors' binding sites. This may explain why the strong binding computed for compound **2** failed to translate into potent cytotoxicity against the HeLa cell line.

To identify which of the protein-inhibitor systems best reproduced the experimentally-observed inhibition, a correlation of the obtained binding energetics against IC_{50} values was performed.

Three MAP kinases, MAPK1 (correlation coefficient of 0.71), MAPK8 (correlation coefficient of 0.67) and MAPK3 (correlation coefficient of 0.60) produced significant correlation patterns (Table 1). Interestingly, inhibition of the three MAP kinases have been implicated in anticancer activity of other natural products.[38,39] In other words, while the experimentally-observed inhibitory effects of the compounds may not be fully explained by their binding to the computationally-examined targets in the present work, the obtained analysis strongly suggests somewhat significant roles for the three kinases in the obtained inhibition. It is not inconceivable to expect the inhibitors to bind and interact with a much wider network of molecular targets relevant to cancer, in which case the inhibition observed *in vitro* represents a gross averaging of the cumulative binding and inhibitory effects at several molecular targets. As such, employing multiple targets in analysis, as has been performed in this work, provides a more robust description of the molecular events resulting in cytotoxic potencies. Analysis of the specific interactions for MAPK1 reveals a plurality of binding site interactions for the different compounds (Figure 4, Figure 5 and Figure 6). Doxorubicin, for instance, relies on extensive network of hydrophobic contacts involving amino acid residues like Ile29, Val37, Gln103, Met106, Thr108, Ser151, Leu154 and Cys164 (Figure 6). Compound **2** additionally recruits multiple directional hydrogen bonds with Met106, Glu69 and Asp165, which translates into a stronger binding site interaction as revealed in the resulting energetics (Figure 5). Compound **1** in addition to multiple hydrophobic contacts also formed hydrogen bond with the amide nitrogen of Ala33, employing one of the hydroxyl groups present in the molecule (Figure 5). Compound **3** formed no hydrogen bonds, a phenomenon that partially resulted from the absence of proton donors in the structure (Figure 4). The strength of its hydrophobic interactions can be highlighted by noting that a more favourable energetic was obtained (-6.4 kcal), compared with compound **4**

(Figure 4) which formed three hydrogen bonds (-5.4 kcal) (Table 1). By relying on both hydrogen bond and extensive hydrophobic contacts, therefore, compound **1** was able to interact with critical amino acid residues in the binding site of MAPK1, which we believe contributes, at least in part, to its profile of inhibition observed in the cell viability assay.

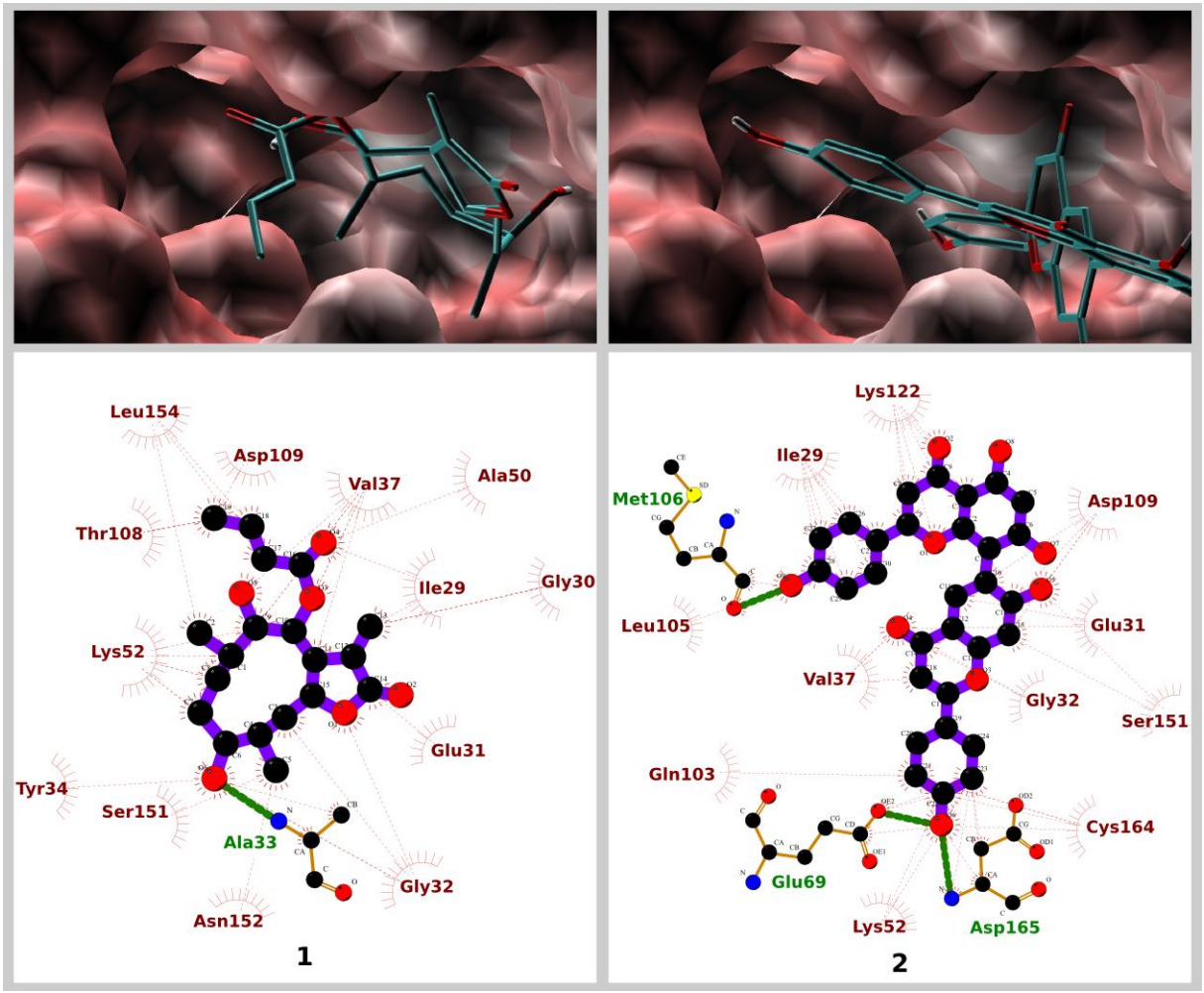

Figure 4. *Top*: Surface representation of bound zoapatanolide A (**1**) (left) and agathisflavone (**2**) (right) within the MAPK1 binding site. *Bottom:* Binding site interactions, with thin dashed lines indicating hydrophobic contacts and the thicker green lines showing hydrogen bonding with zoapatanolide A (**1**) (left) and agathisflavone (**2**) (right).

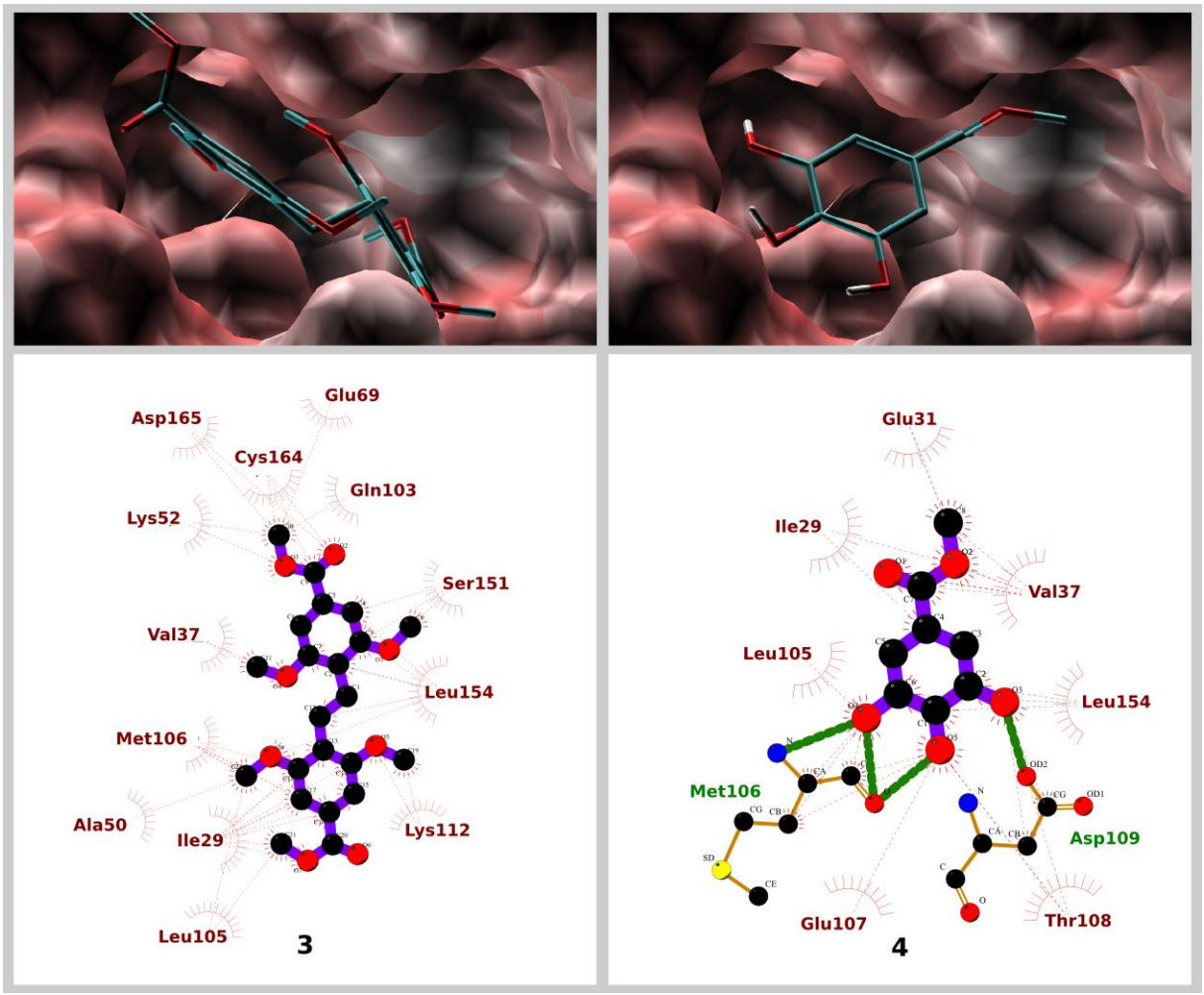

Figure 5. *Top*: Surface representation of bound anacardicin (**3**) (left) and methyl gallate (**4**) (right) within the MAPK1 binding site. *Bottom*: Binding site interactions, with thin dashed lines indicating hydrophobic contacts and the thicker green lines showing hydrogen bonding with compounds anacardicin (**3**) (left) and methyl gallate (**4**) (right).

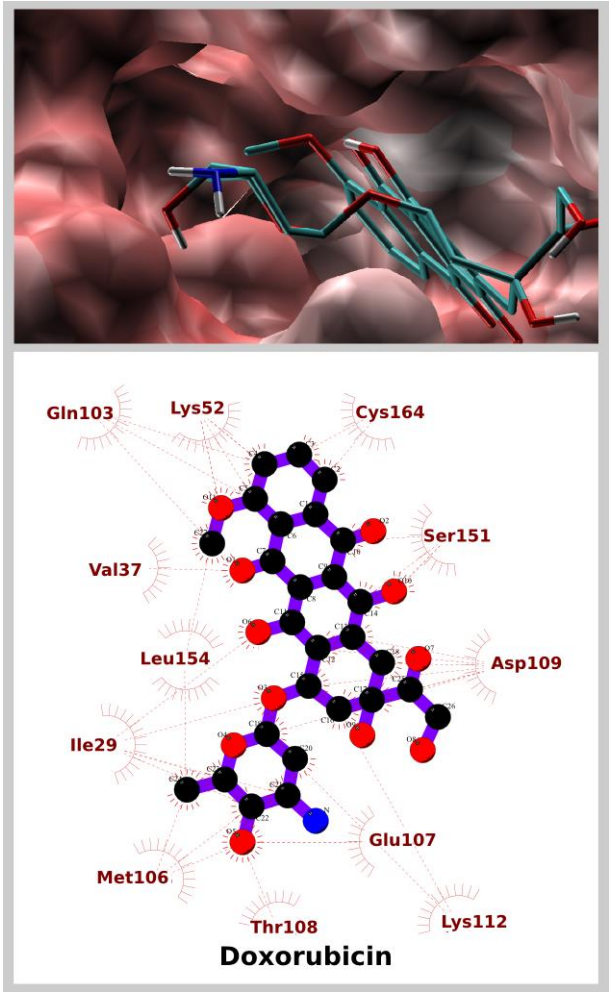

Figure 6. *Top*: Surface representation of bound doxorubicin within the MAPK1 binding site. *Bottom*: Binding site interactions, with thin dashed lines indicating hydrophobic contacts and the thicker green lines showing hydrogen bonding.

Compound	IC_{50} (μM)	Binding free energy (kcal/mol)						
		MAPK8	MAPK10	MAP3K12	MAPK3	MAPK1	VEGF	MAPK7
1	36.2	-6.4	-7.0	-6.6	-8.2	-7.1	-6.8	-4.6
2	84.7	-7.9	-9.9	-8.6	-11.3	-8.3	-10.8	+3.6

3	46.5	-6.4	-7.4	-6.3	-7.8	-6.4	-6.9	-6.0
4	267.2	-5.5	-5.8	-6.1	-6.0	-5.4	-5.6	-5.9
Doxorubicin	2.3	-8.4	-7.5	-7.8	-9.5	-7.9	-9.2	-6.3
$P_{e.i.}$	1.0000	0.67*	0.45	0.41	0.60*	0.71*	0.50	-0.03

Table 1. Autodock Vina binding free energies and Pearson correlation coefficients with experimentally-obtained IC_{50} values. The asterisked correlation coefficients indicate significant correlation patterns.

2.5. Nigerian medicinal plants as a source of lead compounds

Information about curative effects of Nigerian medicinal plants and recipes used by traditional medical practitioners (TMPs) to treat various diseases is difficult to obtain due to many factors, including perceived lack of trust between the TMPs and the scientists. Many of the custodians of the indigenous knowledge are old and a lot of information is being lost due to lack of documentation. The plant investigated in this study was chosen based on volunteered information from a TMP. Ashidi *et al.*[24] concluded that the TMPs do have good understanding of the cancerous disease conditions and of the treatment outcomes. This study of one of the constituent plants in the volunteered recipe indicates that the plant has potential antitumour activity. Four compounds were isolated from the plant. One of them, the biflavonoid agathisflavone, had been reported to have antiproliferative activity against Jurkat cells, with an IC_{50} value of 4.45 μM,[40] with apoptosis as its main mechanism of action. The much higher IC_{50} value (lower potency) obtained in our study could be attributed to differences in cell types used, as the study that reported the antiproliferative activity of agathisflavone on Jurkat cells found that

its strong effect was cell-specific, as it showed modest or marginal cytotoxicity in the other cell lines (HL60, Raji, Hep-2) tested. The study also assessed cell proliferation using tritiated thymidine (radioligand) incorporation assay, whereas we assessed cell viability through a fluorescence-based method. In our study, the most potent of the compounds, zoapatanolide A is a sesquiterpene α-methylene-γ-lactone, a class of compounds which have been found to act as a Michael acceptor for the thiol group of cysteines in proteins, thereby modifying the protein covalently.[41,42,43] The other compounds are anacardicin and gallic acid. While many salicylic acid derivatives with cytotoxic activities have been isolated from the juice of *A. occidentale,*[44] this work is the first to report the isolation of zoapatanolide A, a sesquiterpene α-methylene-γ-lactone, and anacardicin from the leaf extract of *A. occidentale* and explore the possible molecular basis for their observed cytotoxic activities.

In the future, however, we would want to assess their effects on both cancer and normal cells, in order to know whether they can discriminate between these cells, which, if they can, will even further enhance their prospect for development as anticancer agents. However, as each pure compound was not very potently cytotoxic, we consider that the potential synergistic interactions of the compounds with one another as well as with the constituents of the other plants in the herbal formulation are likely to be very important and thus also warrant future studies.

3. Conclusion

A. occidentale contains compounds with some cytotoxic activity, which might justify its inclusion in Nigerian herbal recipes for the management of cancer. Thus, Nigerian medicinal plants represent a veritable source of lead compounds for cancer drug discovery and development.

4. Material and Methods

4.1. General

^{1}H and ^{13}C NMR spectra (for both 1D and 2D experiments) were obtained on the Bruker AV400 (IconNMR) Spectrometer at 400 and 100 MHz, respectively, while the LCMS analyses were carried out on an Agilent LC-MS comprising a 1100 series LC/MSD Trap SL at the Analytical Center of the University of Bradford, United Kingdom. The HRMS data for Compound **1** (zoapatanolide A) were acquired at the Engineering and Physical Sciences Research Council (EPSRC) National Mass Spectrometry Facility, College of Medicine, Groove Building, Swansea University, Swansea, UK, and at Pietermaritzburg Mass Service, School of Chemistry and Physics, University of Kwazulu-Natal, South Africa. Adsorption chromatography (open column) was performed with Kieselgel 60 (ASTM 230–400 mesh, Merck). Size exclusion column chromatography was achieved on Sephadex LH-20 (Pharmacia) pre-swollen in specified solvent before loading onto the column. All thin-layer chromatographic (TLC) analyses were performed at ambient temperature using analytical silica gel 60 GF_{254} pre-coated aluminum backed plates (Merck, 0.25 mm thick). The resulting spots on TLC plates were visualized under UV light (254 nm) and detected by the use of 1% vanillin/H_2SO_4.

4.2. Collection of the plants vegetative parts

The leaves of *Anacardium occidentale* (FPI 2107) were collected on Road 9, Obafemi Awolowo University Staff quarters in April 2014. The plant's vegetative parts were identified by Mr. A.A. Ogunlowo of the Department of Pharmacognosy and deposited in the IFE Herbarium. The leaves were air-dried at room temperature and powdered.

4.3. Fractionation of the crude extract and isolation of compounds from A. occidentale

The powdered leaves (1.6 kg) were extracted with absolute ethanol (5 x 2.5 L) for two days and the crude extract was concentrated *in vacuo* to yield 380 g. The crude extract was dissolved in 500 mL of water and the solution was subjected to acetone precipitation by adding 100% acetone (2.5 L) until precipitate started coming out and it was left for six hours. The supernatant (acetone soluble fraction) was concentrated to dryness *in vacuo* to give 80 g. The precipitate yielded 246 g. Only the acetone-soluble fraction inhibited viability of Hela cells and was therefore fractionated on silica gel (mesh 230-400, column 30 x 5 cm) using solvent mixtures of increasing polarities from 100% $CHCl_3$ through 100% EtOAc to 100 % MeOH. About 20 mL of the eluate was collected into each test tube. The contents of the test tubes were analyzed on TLC using the following solvent mixtures as mobile phases: 100% $CHCl_3$, $CHCl_3$-EtOAc (1:1), 100% EtOAc, EtOAC-MeOH (9:1), EtOAc-MeOH-H_2O-AcOH (10:2:1:0.2) and BuOH-MeOH-H_2O (6.5:3.5:1). Each chromatogram was viewed under the UV lamp at both 254 and 366 nm and was sprayed with 10% sulfuric acid in methanol. Test tubes with similar TLC profiles were combined to give fractions (AO is an abbreviation for *A. occidentale*) AO1 (11.0 g), AO2 (1.5 g), AO 3 (21.1 g), AO 4 (12.9 g), AO 5 (14.9 g) and AO 6 (11.2 g). All the fractions were subjected to the Alamar blue-based cell viability assay as already described in this paper. Only fraction AO 2 elicited toxicity in Hela cells. This was fractionated further on silica gel mesh 230-400 using an open column (20 x 2 cm) with gradient elution starting with 100% $CHCl_3$ through 100% EtOAc to 40% MeOH. Eluates of about 10 mL were collected in small sample bottles and were analyzed on TLC with 100% EtOAc as mobile phase. Test tubes with similar TLC profiles were combined give AO 2A (0.094 g), AO 2B (0.028 g), AO 2C (0.034 g), AO 2D (0.469 g), AO 2E (0.189 g)

and AO 2F (0.745 g). Only AO 2A (eluted with 10% EtOAc in $CHCl_3$), AO 2B (eluted with 30% EtOAc in $CHCl_3$) and AO 2F (eluted with 10-30% MeOH in EtOAc) showed toxicity against Hela cells. Fraction AO 2F with relatively good weight was therefore repeatedly subjected to isocratic elution using 5% MeOH in EtAOc to give agathisflavone (**2)** (0.242 g, 0.015% w/w**),** zoapatanolide A (**1**) (0.120 g, 0.0075% w/w**),** anacardicin (**3**) (0.043 g, 0.0027% w/w) and methyl gallate (**4**) (0.196 g, 0.012% w/w) as pure compounds.

4.4. Cell viability assay and microscopy

HeLa cells were plated into black, flat-bottomed 96-well plates at a density of 1 x 10^5 cells/mL (100 µl/well)[45] using as the growth medium Minimum Essential Medium (MEM) supplemented with 10% Foetal Bovine Serum (FBS), 1% non-essential amino acid (NEAA), glutamine (2 mM) and 1% antibiotic-antimycotic solution. The cells were incubated for 24 h at 37 ºC in a humidified atmosphere of 5% CO_2 before they were exposed to a range of concentrations of the test compounds for 48 h. Alamar Blue (AB) was used to quantify cell viability as previously described (3 h of incubation with AB, cooling plates to room temperature and reading plates (fluorescence excitation at 530 nm (544 nm used), emission at 590 nm) on FlexStation 3 (Molecular Devices)) [41.] Values for compound-treated wells were compared with those of control wells that were treated with DMSO only. Control values were then set at 100% and values for the compound-treated wells were normalized to the control values. Changes to the morphology of the cells induced by test compounds were monitored on a Nikon Eclipse TS 100 inverted microscope fitted with a camera.

4.5. Data analysis

Values are shown as Mean ± SEM (standard error of the mean). Statistical analysis was done using GraphPad (Version 7.01, GraphPad Software, Inc., CA, USA). One-way analysis of variance (ANOVA) was used to compare the differences between means, followed by Dunnett's multiple comparisons test (comparison of each treatment mean to the control mean). A p-value of <0.05 was considered statistically significant. To calculate IC_{50} values, viability data were fit to the non-linear regression equation log (inhibitor) versus response - variable slope (four parameters).

4.6. Computational modeling

There are several molecular targets implicated in cancer development with which a compound demonstrating anticancer property can bind to. In this study, rather than employ a single molecular target, we have employed seven different proteins. Six of these (including MAPK8, MAPK10, MAP3K12, MAPK3, MAPK1 and MAPK7) are mitogen-activated protein kinases involved in growth and cell proliferation, differentiation, apoptosis and migration[46], while the seventh is the vascular endothelial growth factor (VEGF) that is important in angiogenesis and metastasis by extension[47]. High-resolution crystal structures of inhibitor-protein complexes corresponding to MAPK8, MAPK10, MAP3K12, MAPK3, MAPK1 and MAPK7 and VEGF were downloaded from the RCSB database and with accession codes and resolution 4QTB. PDB : 1.4 A, 4ZZN.PDB ; 1.33 A, 4ZSG.PDB ; 1.79 A, 4QTD.PDB ; 1.50 A, 4W4W.PDB ; 1.90 A, 5CEP.PDB ; 1.99 A, and 3WZD.PDB ; 1.57 A, respectively. Coordinates of the inhibitors were removed from the complexes after which docking grids were generated using AutoDock Tool[48,49] focusing on the binding site residues as identified in the crystallographic structures. Following

this, AutoDock Vina[50] was employed in docking each of the energy-minimized 3D structures (treated as flexible) of zoapatanolide A (**1**), agathisflavone (**2**), anacardicin (**3**), methyl gallate (**4**) and doxorubicin against each of the seven protein receptors (treated as rigid). An exhaustiveness of 4 was employed. The computed binding free energies and structures for the top conformations were saved for post-docking analysis. To gain an insight into the likely molecular basis of the observed cytotoxic effects of the investigated compounds, Pearson correlation coefficient was calculated using the formula:

$$P_{\mathrm{e.i}} = \frac{\left(\frac{1}{N}\sum_{\mathrm{i}=1}^{N}(e_i - \bar{e})\,(i_i - \bar{\imath})\right)}{\left(\sqrt{\left(\frac{1}{N}\sum_{\mathrm{i}=1}^{N}(e_i - e)^2\right)} \times \sqrt{\left(\frac{1}{N}\sum_{\mathrm{i}=1}^{N}(i_i - i)^2\right)}\right)}$$

where the numerator captures the sample variance. The two denominators represent the standard deviations for the computed binding energy (e) and the experimentally-observed IC_{50} value (i), while their mean values are denoted with $\bar{e}$ and $\bar{\imath}$, respectively. Finally, to better understand the relationship between the Vina-computed binding free energies and the observed cytotoxicity, molecular descriptors (logP(o/w), number of hydrogen bond acceptors and donors and molecular weight were computed using molecular operating environment.[51]

Funding

This work was supported by a British Council Researcher Links Travel Grant 2013 to TBJ, a South Africa National Research Foundation (NRF) Grant No 98345 (2016) to FRVH and an academic staff funding provided to AAF by the School of Pharmacy, University of Bradford, UK.

Acknowledgments

MS data were acquired at the EPSRC UK National Mass Spectrometry Facility at Swansea University, UK, for which we gratefully acknowledge the assistance provided. The financial support given to TBJ and AAF by the School of Pharmacy, University of Bradford, UK, under the leadership of Professor Marcus Rattray, is duly appreciated. TBJ wishes to use this paper to acknowledge Prof. A.O. Ogundaini, Professor of Pharmaceutical Chemistry, on the occasion of his 60th birthday, for his contributions to natural product chemistry research in Africa.

References

1. http://www.cancer.org/Research/CancerFactsFigures/CancerFactsFigures/index (accessed January 19, 2017).

2. The Global Burden of Disease Cancer Collaboration. *JAMA Oncol.* **2015**, *1*, 505-527.

3. Global Burden of Disease 2013 Mortality and Causes of Death Collaborators. *Lancet* **2015**, *385*, 117-171.

4. Pledgie-Tracy, A.; Sobolewski, M.D.; Davidson, N.E. *Mol. Cancer Ther*. **2007,** *6*, 1013-1021.

5. Amin, A.; Gali-Muhtasib, H.; Ocker, M.; Schneider-Stock, R. *Int. J. Biomed. Sci.* **2009,** *5*, 1-11.

6 Desai, A.G.; Qazi, G.N; Ganju, R.K.; El-Tamer, M.; Singh, J.; Saxena, A.K.; Bedi, Y.S.; Taneja, S.C.; Bhat, H.K. *Curr Drug Metab*. **2008** *9,* 581–591.

7. Unnati, S.; Ripal, S.; Sanjeev, A.; Niyati, A. *Chin. J. Nat. Med.* **2013,** *11,* 0016-0023.

8. Amos, L.A.; Löwe, J. *Chem. Biol*. **1999,** *6,* 65-69.

9. Jordan, M.A.; Wilson, L. *Nat. Rev. Cancer*. **2004,** *4,* 253-266.

10. Khazir, J.; Mir, B.A.; Pilcher, L.; Riley, D.L. *Phytochem. Lett.* **2014,** *7,* 173-181.

11. Solowey, E.; Lichtenstein, M.; Sallo, S.; Paavilainen, H.; Solowet, E.; Lorberboum-Galski, H. *Scientific World J.* **2014,** *2014,* 1-12.

12. Pezzuto, J.M. *Biochem. Pharmacol.* **1997,** *53,* 121-133.

13. Cragg, G.M.; Newman, D.J. *J. Ethnopharmacol.* **2005,** *100,* 72-79.

14. Boyle, P.; Levin, B. International Agency for Research on Cancer, France. **2008,** *48*.

15. Wani, M.C.; Taylor, H.L.; M.E.; Coggon, P.; McPhail, A.T. *J. Am. Chem. Soc.* **1971**, *93,* 2325-2327.

16. Loike, J.D.; Brewer, C.F.; Sternlicht, H.; Gensler, W.J.; Horwitz, S.B. *Cancer Res.* **1978,** *38,* 2688-2693.

17. Meijer, W.; *Econ. Bot*. **1974,** *28,* 68-72.

18. Noble, R.L. *Biochem. Cell Biol.* **1990,** *68,* 1344-1351.

19. Zhang, Y.; Talalay, P.; Cho, C.G.; Posner, G.H. *Proc. Natl. Acad. Sci. USA.* **1992,** *89,* 2399-2403.

20. Papi, A.; Orlandi, M.; Bartolini, G.; Barillari, J.; Iori, R.; Paolini, M.; Ferroni, F.; Fumo, M.G.; Pedulli, G.F.; Valgimigli, L. *J. Agric Food Chem.* **2008,** *56,* 875-883.

21. Pettit, G.R.; Singh, S.B.; Niven, M.L.; Hamel, E.; Schmidt, J.M. *J. Nat. Prod.* **1987,** *50* 119-131.

22. Oladele, A.T.; Alade, G.O.; Omobuwajo, O.R. *Agric. Biol. J. North Amer.* **2011,** *2* 476-487.

23. Sowemimo, A.; Van de Venter, M.; Baatjies, L.; Koekemoer, T. *J. Med. Plants Res.* **2011,** *5,* 2442-2444.

24. Ashidi, J.S.; Houghton, P.J.; Hylands, P.J.; Efferth, T. *J. Ethnopharmacol.* **2010,** *128,* 501-512.

25. Soladoye, M.O.; Amusa, N.A.; Raji-Esan, S.O.; Chukwuma, E.E.; Taiwo, A.A. *Annals Biol. Res.* **2010,** *1*, 261-273**.**

26. Abubakar, M.S.; Musa, A.M.; Ahmed, A.; Hussaini, I.M. *J. Ethnopharmacol.* **2007,** *111*, 625-629.

27. Taiwo, B.J.; Taiwo, G.O.; Olubiyi, O.O.; Fatokun, A.A. *Bioorg. Med. Chem. Lett.* **2016,** *26*, 3404-3410.

28 Quijano, L.; Gomez-G, F.; Sierra-R, E.; Rios, T. *Phytochemistry.* **1991, *30*,** 1947-1950.

29 Quijano, L.; Gomez-G, F.; Calderon, J.S.;Lopez-P, J.; Rios, T. *Phytochemistry.* **1984** *23,* 125-127.

30. Quijano, L.; Calderon, J.S.; Gomez, F.; Rios, T. *Phytochemistry* **1982,** *21,* 2041-2044.

31. Ajileye, O.O.; Obuotor, E.M.; Akinkunmi, E.O.; Aderogba, M.A. *J. King Saud University – Sci.* **2015,** *27,* 244-252.

32. Svenningsen, A.B.; Madsen, K.D.; Liljefors, T.; Stafford, G.I.; van Staden, J.; Jager, A.K. *J. Ethnopharmacol.* **2006,** *103,* 276-280.

33. Battersby, A.R.; Binks, R. *J. Chem. Soc.* **1955,** 2888-2895.

34. Kamatham, S.; Kumar, N.; Gudipalli, P. *Toxicol. Rep.* **2015,** *2*, 520-529.

35. Hall, I.H.; Lee, K.H.; Starnes, C.O.; Eigebaly, S.A.; Ibuka, T.; Wu, K-S.; Kimura, T.; Haruna, M. *J. Pharm. Sci.* **1978,** *67*, 1235-1238.

36. Villagomez, R.; Collado, J.A.; Munoz, E.; Almanza, G. ; Sterner, O. *J. Biomed. Sci. Eng.* **2014,** *7,* 833-847.

37. Maldonado, E.M.; Svensson, D.; Oredsson, S.M.; Sterner, O. *Sci. Pharma.* **2014,** *82,* 147-160.

38. Jeong, J.J.; Jang, S.E.; Hyam, S.R.; Han, M.J.; Kim, D.H. *Eur. J. Pharmacol*. **2014**, *740*, 652-661.

39. Li, J.; Malakhova, M.; Mottamal, M.; Reddy, K.; Kurinov, I.; Carper, A.; Langfald, A.; Oi, N.; Kim, M.O.; Zhu, F.; Sosa, C.P.; Zhou, K.; Bode, A.M.; Dong, Z. *Cancer Res*. **2012**, *72,* 260-270.

40. Konan, N.A.; Lincopan, N.; Díaz, I.E.; de Fátima Jacysyn, J; Tiba, M.M., Amarante Mendes, J.G.; Bacchi, E.M.; Spira, B. *Exp. Toxicol. Pathol.* **2012**. *64*, 435-440.

41. Scotti, M.T.; Fernandes, M.B.; Ferreira, M.J.P.; Emerenciano, V.P. *Bioorg. Med. Chem.* **2007,** *15,* 2927-2934.

42. Picman, A.K. *Biochem. Syst. Ecol.* **1986,** *14,* 255-281.

43. Zhang, S.; Won, Y-K.; Ong, C-N.; Shen, H-M. *Curr. Med. Chem. Anticancer Agents* **2005**, *5,* 239-249.

44. Kubo, I.; Ochi, M.; Vieira, P.C.; Komatsu, S. *J. Agric. Food. Chem.* **1993,** *41,* 1012-1015.

45. Fatokun, A.A.; Liu, J.O.; Dawson, V.L.; Dawson, T.M. *Brit. J. Pharmacol.* **2013**, *169*, 1263-1278.

46. Santarpia, L.; Lippman, S.M.; El-Naggar, A.K. *Expert Opin Ther Targets* **2012**, *16*, 103-119.

47. Hanahan D.; Weinberg, R.A. *Cell* **2011**, *144*, 646-674.

48. Goodsell, D.S.; Morris, G.M.; Olson, A.J. *J Mol Recognit.* **1996**, *9*, 1-5.

49. Santos-Martins, D.; Forli, S.; Ramos, M.J.; Olson, A.J. *J. Chem. Inf Model.* **2014,** *54,* 2371-2379.

50. Trott, O.; Olson, A.J. *J. Comput. Chem.* **2010,** *31,* 455-461.

51. Molecular Operating Environment (MOE), 2013.08; Chemical Computing Group Inc., 1010 Sherbooke St. West, Suite #910, Montreal, QC, Canada, H3A 2R7, 2017.